Ab Initio Study on the $(OCS)_2 \cdot CO_2$ van der Waals Trimers

H. Valdés and J. A. Sordo*

Laboratorio de Química Computacional, Departamento de Química Física y Analítica, Facultad de Química, Universidad de Oviedo, Julián Clavería 8, 33006 Oviedo, Principado de Asturias, Spain

Received: July 23, 2001; In Final Form: February 6, 2002

Ab initio calculations [MP2, MP4SDTQ, and QCISD(T)] using different basis sets [6-31G(d,p), cc-pVXZ (X = D, T, Q), and aug-cc-pVDZ] were carried out to study the $(OCS)_2 \cdot CO_2$ van der Waals trimers. Three barrel-like structures [C_1 (two) and C_2 symmetry] and three planar (C_s) structures were located on the potential energy surface. Their CBS-MP2/cc-pVXZ (X = D, T, Q) stabilization energies are 1760 (C_1), 1514 (C_2), 1660 (C_1), 1325 (C_s), 1556 (C_s), and 1398 (C_s) cm^{-1}, respectively. The most stable structure (one of the C_1 barrel-like isomers) has bond lengths, angles, rotational constants, and dipole moment that agree quite well with the corresponding experimental values of the only structure observed in recent microwave spectroscopic studies. The energetic proximity of the rest of the isomers strongly suggests that the experimentally unobserved structures might also be present in the supersonic adiabatic expansion of the gas in the microwave spectroscopic studies as in the case of the $(CO_2)_3$ trimer where both barrel-like and planar isomers have been reported to exist. The many-body symmetry-adapted perturbation theory helps to shed some light on the nature of the interactions leading to the formation of the different isomers. While the dispersion forces make the most important attractive contributions to the interaction energies of the $(OCS)_2 \cdot CO_2$ isomers, the induction forces make contributions similar in magnitude to the electrostatic forces. The three-body contributions are small and stabilizing for the barrel-like structures and are less important for the cyclic isomers.

Introduction

The field of cluster research has been growing in interest during the past decades as a consequence of spectacular advances in high-resolution spectroscopic techniques using supersonic expansions and the advent of the laser, which enabled detailed spectroscopic observations through the probing of systems of varying size.[1] From the theoretical viewpoint, the impressive parallel developments of computer technology and electronic structure theory[2] favored the study of clusters for which the weakness of the interactions and the nature of the forces involved require, in general, the use of computational high-cost methodologies.

Needless to say, the synergistic interaction between theory and experiment led to the significant advances made in recent years. In this context, the notable progress in the field becomes evident when realizing that three of the papers in the Centennial Issue published in 1996 by *The Journal of Physical Chemistry* were devoted to cluster research.[1,3,4]

Particularly, the study of weakly bound van der Waals complexes and hydrogen-bonded systems has deserved special attention as demonstrated by the fact that in the past 13 years three issues of *Chemical Reviews* have been fully devoted to the subject.[5−7] The analysis of the nature of the forces involved in the formation of such complexes is of fundamental importance to gaining a deeper understanding of bulk materials, a subject of value not only in chemistry and physics, but also in biology.

After a long period of time where research was focused on the study of dimer structures, in the past decade a growing number of studies on weakly bound trimers have been reported. Particularly, Kuczkowski and Peebles have recently analyzed the rotational spectra of a number of trimers using pulsed-nozzle Fourier transform microwave spectroscopy techniques.[8] Structural information from these works allowed the authors to conclude that the trimers are often composed of sets of dimer-type structures, although with subtle differences in the angles and/or lengths. On the other hand, the application of semiempirical models based on distributed electrostatic interactions and improved by the inclusion of dispersion−repulsion terms[9] has proved to be quite useful for providing initial assignments of the rotational spectrum and for explaining and rationalizing trimer properties by comparison with dimer interactions.[10]

Although the ab initio methodologies are certainly less amenable to the study of larger weakly bonded systems, Chalasinski and Szczesniak concluded recently[11] that the aforementioned impressive advances in computational chemistry demonstrated that the supermolecular approach based on the Moller−Plesset perturbation[12] and coupled-cluster theories,[13] along with the symmetry-adapted perturbation theory,[14] is capable of providing the rigorous, quantitative, and physically meaningful description of intermolecular forces. Recent work from our laboratory on hydrogen-bonded systems[15−18] and van der Waals complexes[19−22] fully corroborates the above conclusion.

In a recent article,[10] Peebles and Kuczkowski reported the structure and dipole moment of the $(OCS)_2 \cdot CO_2$ trimer from microwave spectroscopic experiments. The authors showed that the deduced structure can be closely reproduced by Stone et al.'s ORIENT program,[23] which implements a semiempirical model incorporating electrostatic, dispersion, and repulsion interactions.

In the present work, we report the results of an ab initio study, including both supermolecular and perturbational treatments, on the $(OCS)_2 \cdot CO_2$ trimer. Our goal is 2-fold: on one hand, the analysis of the theoretical results will shed additional light on the nature of the forces involved in the formation of the

* Corresponding author. Fax: +34 985237850. E-mail: jasg@correo.uniovi.es.

10.1021/jp0128168 CCC: $22.00
Published on Web 03/23/2002

trimer. On the other hand, we hope the information provided will be helpful for planning further experimental work. Particularly, the structural information can be used to generate initial assignments of the transitions corresponding to unobserved structures that according to energy considerations are likely to be present in the molecular beam.

Theoretical Methods

Supermolecular perturbational and variational methodologies were employed to explore the potential energy surface (PES) of the $(OCS)_2$·CO_2 system and to estimate the energies of all the structures on it. On the other hand, the symmetry-adapted perturbation theory (SAPT) was used to gain insight into the physical nature and magnitude of the forces responsible for the formation of the trimer structure.

Supermolecular Calculations. We first carried out an exhaustive exploration of the PES at the second-order Moller−Plesset perturbation theory (MP2) level employing different basis sets. Optimizations with Pople's 6-31G(d,p)[12] and Dunning's[24,25] cc-pVDZ, cc-pVTZ, and aug-cc-pVDZ correlation-consistent basis sets were performed. The latter (augmented) basis, which includes s, p, and d diffuse functions, was specially designed to deal with systems where correlation contributions are expected to play a relevant role.[25,26] Indeed, Sponer and Hobza have recently stressed[27] the good performance of the aug-cc-pVDZ basis set to estimate the dispersion contributions in weakly bound complexes. As concluded by different authors[26,28] and in agreement with our own previous experience,[15−22] these levels of theory provide reliable structural information on weakly bound molecules. Density functional theory (DFT) calculations with Becke's three-parameter exchange functional[29] and the correlation functional of Lee−Yang−Parr[30] (B3LYP) were also accomplished. As expected, the DFT methodology was not capable of reproducing the experimental results as a consequence of the well-known fact[31,32] that the available functionals do not represent properly the London dispersion component of the interaction energy which, as we will show below (see in the next sections the analysis of the SAPT results collected in Tables 6 and 7), is of paramount importance for the systems under study. The DFT/B3LYP results are available as Supporting Information.

To improve the energetic predictions, MP4SDTQ//MP2 and QCISD(T)//MP2 calculations using 6-31G(d,p), cc-pVDZ, and aug-cc-pVDZ basis sets were performed. It is well-known[33] that the QCISD(T) level provides energy predictions quite similar to the ones obtained with the CCSD(T) method, and this latter level has been shown to reproduce quite well, in general, the CCSDT energetic results.[26,34−36] Therefore, the QCISD(T)//MP2 energies computed in this work should be reliable.

In a very recent review,[31] Müller-Dethlefs and Hobza stressed that the inclusion of counterpoise corrections (CP)[37] for basis set superposition error (BSSE) is a controversial point. Indeed, while some authors claimed that the CP algorithm is a rigorously correct procedure at any level of theory,[38] a number of authors reported overcorrected values for the energies computed using the CP algorithm at the correlated level.[39] In this work, we will analyze the CP estimates of the BSSE for the OCS·OCS and OCS·CO_2 dimers (both isolated and forming part of the trimers). Comparison between the CP corrected interaction energies and the corresponding BSSE-free values arising from the symmetry-adapted perturbation theory formalism[40] (see below) will allow us to provide further data of interest in the debate about the CP overcorrection.

Further problems arise from the fact that the application of the CP method in the case of trimer or larger clusters is not straightforward. Indeed, several recipes leading to different results can be applied.[41] To circumvent this difficulty, we carried out estimations of the stabilization energies of the trimers at the complete basis set (CBS) limit by exploiting the regular behavior observed by the energies obtained with a series of correlation-consistent basis sets through the use of a mixed exponential/Gaussian function of the form[42]

$$E(x) = E_{\mathrm{CBS}} + B\exp[-(x-1)] + C\exp[-(x-1)^2] \quad (1)$$

Although several alternate expressions are available, our previous experience[35] showed that no significant differences arise from the different extrapolation models. The CBS extrapolations were carried out from MP2/cc-pVXZ (X = D, T, Q) calculations. (Since MP2/cc-pVQZ optimizations, involving 503 basis functions, are computationally prohibitive, we used MP2/cc-pVQZ//MP2/cc-pVTZ energies in the extrapolations.) By definition, the CBS extrapolations are BSSE-free, thus providing us with a procedure to make reliable predictions on stabilization energies for the trimer isomers considered in the present work.

All the supermolecular calculations were carried out with the Gaussian 98 packages of programs.[43]

To characterize the interactions responsible for the formation of the trimers, we carried out a Bader topological analysis[44] of the corresponding charge densities. The location of the critical points (r_c) and the magnitude of the electronic density [$\rho(r_c)$], Laplacian of electronic density [$\nabla^2\rho(r_c)$], and energy density [$H(r_c)$] at them provide valuable information on the atoms involved in the binding and the nature of the interactions between the different dimers into the trimer.[45] (The computed values for all these magnitudes are available as Supporting Information.)

Symmetry-Adapted Perturbation Theory (SAPT) Calculations. A detailed account of the many-body symmetry-adapted perturbation theory (SAPT) approach can be found in refs 40 and 46−49, where the details on its implementation in a computer code (SAPT96) are also given.

In the SAPT formalism, the interaction energy, E_{int}(SAPT), is calculated as

$$E_{\mathrm{int}}(\mathrm{SAPT}) = E_{\mathrm{int}}^{\mathrm{HF}} + E_{\mathrm{int}}^{\mathrm{CORR}} \quad (2)$$

where $E_{\mathrm{int}}^{\mathrm{HF}}$ represents the supermolecular Hartree−Fock (HF) interaction energy

$$E_{\mathrm{int}}^{\mathrm{HF}} = E_{\mathrm{pol}}^{(10)} + E_{\mathrm{exch}}^{(10)} + E_{\mathrm{ind,r}}^{(20)} + E_{\mathrm{exch-ind,r}}^{(20)} + \delta E_{\mathrm{int}}^{\mathrm{HF}} \quad (3)$$

with $\delta E_{\mathrm{int}}^{\mathrm{HF}}$ collecting all higher order induction and exchange corrections contained in $E_{\mathrm{int}}^{\mathrm{HF}}$ and not computed by the SAPT code ("r" indicates that the corresponding term was computed with the inclusion of the coupled HF response of the perturbed system).[40]

$E_{\mathrm{int}}^{\mathrm{CORR}}$ contains the correlated portion of the interaction energy approximated by SAPT as

$$E_{\mathrm{int}}^{\mathrm{CORR}} = E_{\mathrm{pol,r}}^{(12)} + E_{\mathrm{exch}}^{(11)} + E_{\mathrm{exch}}^{(12)} + {}^{\mathrm{t}}E_{\mathrm{ind}}^{(22)} + {}^{\mathrm{t}}E_{\mathrm{exch-ind}}^{(22)} + E_{\mathrm{disp}}^{(20)} + E_{\mathrm{exch-disp}}^{(20)} \quad (4)$$

where the superscript "t" indicates that the true correlation effects,[49] which represent those parts of the $E_{\mathrm{ind}}^{(22)}$ energy that are not included in the term $E_{\mathrm{ind,r}}^{(20)}$ in eq 3, are collected.

TABLE 1: Stabilization Energies (cm^{-1}) for the Three OCS·OCS Dimers Located on the Potential Energy Surface at Different Theoretical Levels[c]

	MP2	MP4SDTQ[b]	QCISD(T)[b]
OCS·OCS (a)[a] 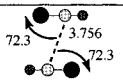			
6-31G(d,p)	510	517	378
cc-pVDZ	534	517	387
aug-cc-pVDZ	887	880	716
cc-pVTZ	660		
OCS·OCS (b) 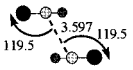			
6-31G(d,p)	596	620	577
cc-pVDZ	472	485	456
aug-cc-pVDZ	698	746	655
cc-pVTZ	534		
OCS·OCS (c) 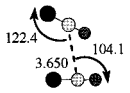			
6-31G(d,p)	540	554	445
cc-pVDZ	539	533	422
aug-cc-pVDZ	788	793	657
cc-pVTZ	604		

[a] Geometric disposition corresponding to the reported experimental geometry (see ref 52). [b] MP4SDTQ//MP2 and QCISD(T)//MP2 values. [c] Some representative geometric parameters (as computed at the MP2/cc-pVTZ level) are also indicated.

TABLE 2: Stabilization Energies (cm^{-1}), Obtained at Different Theoretical Levels for the Two OCS·CO_2 Dimers Located on the Potential Energy Surface[c]

	MP2	MP4SDTQ[b]	QCISD(T)[b]
OCS·CO_2(a)[a] 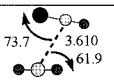			
6-31G(d,p)	501	516	423
cc-pVDZ	550	560	469
aug-cc-pVDZ	691	743	641
cc-pVTZ	531		
OCS·CO_2(b) 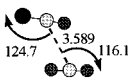			
6-31G(d,p)	612	647	618
cc-pVDZ	527	556	539
aug-cc-pVDZ	631	708	654
cc-pVTZ	505		

[a] Geometric disposition corresponding to the reported experimental complex (see ref 53). [b] MP4SDTQ//MP2 and QCISD(T)//MP2 values. [c] Some representative geometric parameters (as computed at the MP2/cc-pVTZ level) are also indicated.

It can be shown[50] that the results obtained in eq 2 for E_{int}-(SAPT), using eqs 3 and 4, tend asymptotically to the values which would be calculated at the supermolecular MP2 level.

Given the important role which is expected to be played by the dispersion contributions in the weakly bound systems under study (see below), the SAPT calculations reported in this work have been performed using Dunning's aug-cc-pVDZ basis set. (Every calculation for a $(OCS)_2$ dimer took about 24 h running the SAPT96 code[40] on a RISC 6000 workstation with 400 MB RAM.)

Results and Discussion

Isolated Dimers. Peebles and Kuczkowski concluded[10] that, from the growing number of trimer systems that have already been classified, it is becoming apparent that trimers are often composed of sets of dimer-type structures, although with subtle differences in the angles and/or bond lengths. Bearing this point in mind, we performed ab initio calculations to explore the PESs corresponding to the $(OCS)_2$ and OCS·CO_2 dimers.

Tables 1 and 2 collect the energy results for the isomers of the $(OCS)_2$ and OCS·CO_2 dimers located on the PESs at the levels of theory employed in the present work [MP2 optimizations and MP4SDTQ//MP2, QCISD(T)//MP2 single-point calculations]. Linear structures were not considered as they are not expected to play any significant role in the formation of this type of trimers. The most representative geometric parameters (as computed at the MP2/cc-pVTZ level) are also presented.

The PES of the $(OCS)_2$ dimers has been extensively explored by Bone.[51] This author concluded that basis sets of the size of double-ζ with a single shell of polarization functions are inadequate to describe this type of species. The present calculations extend such an observation to the case of the OCS·CO_2 dimer. In fact, the OCS·OCS(a) and OCS·CO_2(a) isomers in Tables 1 and 2 represent geometric dispositions corresponding to the experimentally observed structures.[52,53] As can be seen, the 6-31G(d,p) basis set predicts those structures to be the least stable ones. It is interesting to note that Dunning's cc-pVDZ (of double-ζ size), specially designed to be used in the study of systems where correlation contributions are expected to be relevant, tends to correct the bad performance of the standard 6-31G(d,p) basis, although the QCISD(T)//MP2 single-point predictions using this basis set remain incorrect.

Dunning's aug-cc-pVDZ and cc-pVTZ basis sets correctly predict that the OCS·OCS(a) and OCS·CO_2(a) isomers are the most stable ones. (The exception is the QCISD(T)//MP2 prediction using the aug-cc-pVDZ basis set for the OCS·CO_2 dimer.)

According to Peebles and Kuczkowski,[10] the OCS·OCS(a) and OCS·CO_2(a) dimer structures are expected to play a relevant role in the formation of the $(OCS)_2$·CO_2 trimer. However, as we will show below, one of the most interesting conclusions in the present theoretical study is that the other structures [OCS·OCS(b), OCS·OCS(c), and OCS·CO_2(b) in Tables 1 and 2] are also relevant.

Geometries and Energetics of the Trimers. Figure 1 presents the six minima structures (I−VI) located on the PES for the $(OCS)_2$·CO_2 trimer as computed at the MP2 [with 6-31G-(d,p), cc-pVDZ, aug-cc-pVDZ and cc-pVTZ bases] level of theory. Table 3 collects the most representative structural parameters (bond lengths and angles) and Table 4 contains the corresponding rotational constants and dipole moments. (The Cartesian coordinates are given as Supporting Information.) The stabilization energies for the six trimer isomers are collected in Table 5.

The different basis sets predict rather similar MP2 bond lengths and angles, with the aug-cc-pVDZ basis giving systematically the shortest distances. This behavior is consistent with the fact that the diffuse functions in the augmented basis

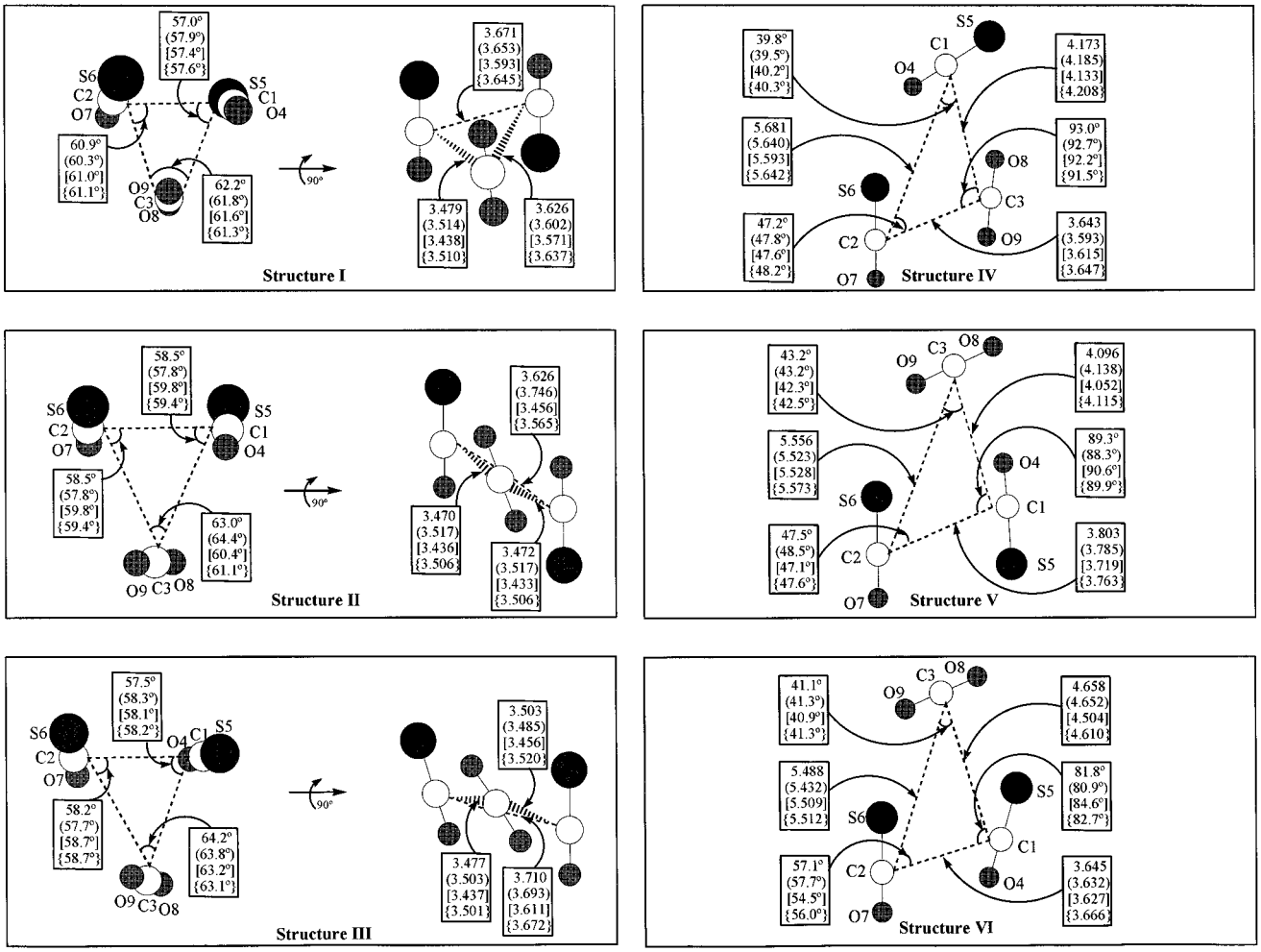

Figure 1. Two views of $(OCS)_2$·CO_2 trimer structures I−VI as computed at the MP2 levels of theory employed in this work: 6-31G(d,p), (cc-pVDZ), [aug-cc-pVDZ], and {cc-pVTZ}. Distances are given in angstroms and angles in degrees. Further structural parameters are given in Table 3 and as Supporting Information.

TABLE 3: MP2/cc-pVTZ Structural Parameters (Distances in Å and Angles in deg)[a] for the $(OCS)_2$·CO_2 van der Waals Complexes

parameter	exptl[c]	structure I	structure II	structure III	structure IV	structure V	structure VI
$r(C_1-C_3)$	3.773(8)	3.637	3.506	3.520	4.208	4.115	4.610
$r(C_2-C_3)$	3.574(6)	3.510	3.506	3.501	3.647	5.573	5.512
$r(C_1-C_2)$	3.757(9)	3.645	3.565	3.672	5.642	3.763	3.666
$r(C_3-M_1)^b$	3.616(9)	3.514	3.799	3.453	4.378	4.617	4.224
$r(C_3-M_2)^b$	3.891(8)	3.803	3.799	3.795	3.502	5.092	5.018
$r(M_1-M_2)^b$	3.652(12)	3.555	4.134	3.817	5.608	3.573	3.819
$\angle(C_2-C_3-C_1)$	61.4(1)	61.3	61.1	63.1	91.5	42.5	41.3
$\angle(O_7-C_2-C_3)$	56.2(7)	59.1	59.4	59.1	109.9	156.9	160.9
$\angle(O_4-C_1-C_2)$	102.3(4)	102.4	62.6	105.2	34.5	107.2	57.0
$\angle(O_8-C_3-C_1)$	60.1(14)	61.5	112.4	66.2	24.9	96.7	91.6
$\tau(O_7-C_2-C_3-C_1)$	133.2(9)	128.7	74.2	68.4	0.0	0.0	0.0
$\tau(O_4-C_1-C_2-C_3)$	−107.4(7)	−103.3	−68.9	94.6	180.0	0.0	180.0
$\tau(O_8-C_3-C_1-C_2)$	−79.0	−77.6	−50.0	133.4	180.0	180.0	180.0

[a] See Figure 1 for structures I−VI. [b] M_i represents the center of mass closer to C_i. [c] See ref 10.

set should contribute to provide a better representation of the (attractive) dispersion forces.[26,27]

In (C_1) structure I (see Figure 1), the two OCS monomers exhibit an antiparallel orientation in an association which is no longer planar. The dihedral angle O7−C2···C1−S5, which should be 0° for a planar configuration (see the OCS·OCS isolated monomers in Table 1), becomes 33° at the MP2/cc-pVTZ level. The planarity of the two OCS·CO_2 fragments (see the OCS·CO_2 isolated monomers in Table 2) is also lost in the trimer; the computed dihedral angles O8−C3···C2−S6 and O9−C3···C1−S5 are 18° and 16°, respectively, at the MP2/cc-pVTZ level. The experimental values for the O7−C2···C1−S5, O8−C3···C2−S6, and O9−C3···C1−S5 dihedral angles are[10] 34°, 20°, and 12°, respectively.

Structure II is quite similar to isomer I with three main differences: (a) it exhibits C_2 symmetry; (b) the two OCS monomers remain in an antiparallel orientation (i.e., with the sulfur atoms pointed in the opposite direction), but they are slipped in such a way that the two oxygens are almost aligned in contrast with structure I where the oxygen atom of each OCS

TABLE 4: Rotational Constants (MHz) and Dipole Moments (D) for the $(OCS)_2 \cdot CO_2$ van der Waals Complexes

	A	B	C	μ
		Structure I		
6-31G(d,p)	1025.1	877.8	627.6	0.379
cc-pVDZ	1037.4	868.8	630.5	0.316
aug-cc-pVDZ	1066.1	907.9	659.4	0.476
cc-pVTZ	1043.0	890.3	640.8	0.419
		Structure II		
6-31G(d,p)	1250.5	685.4	509.4	0.472
cc-pVDZ	1262.2	644.9	485.4	0.355
aug-cc-pVDZ	1184.5	752.1	542.0	0.615
cc-pVTZ	1191.1	715.9	520.6	0.500
		Structure III		
6-31G(d,p)	1177.6	742.5	593.6	1.018
cc-pVDZ	1173.3	751.3	600.2	0.796
aug-cc-pVDZ	1201.1	781.3	627.7	1.245
cc-pVTZ	1169.1	773.8	612.8	1.136
		Structure IV		
6-31G(d,p)	1863.2	439.0	355.3	1.005
cc-pVDZ	1845.1	445.4	358.8	0.724
aug-cc-pVDZ	1879.8	453.6	365.4	1.207
cc-pVTZ	1816.5	447.5	359.0	1.087
		Structure V		
6-31G(d,p)	1215.1	599.7	401.5	0.206
cc-pVDZ	1211.7	601.4	401.9	0.198
aug-cc-pVDZ	1302.8	600.3	411.0	0.182
cc-pVTZ	1257.0	594.1	403.4	0.176
		Structure VI		
6-31G(d,p)	1192.4	622.8	409.1	1.138
cc-pVDZ	1194.3	635.0	414.6	0.885
aug-cc-pVDZ	1324.4	614.1	419.6	1.293
cc-pVTZ	1244.0	617.7	412.8	1.571
exptl[a]	1010.7197 (8)	875.4035 (3)	605.3805 (4)	0.50 (4)

[a] See ref 10.

monomer is aligned with the sulfur atom in the other (see Figure 1); and (c) the CO_2 monomer is more twisted than in structure I. As in the case of structure I, the three dimer fragments are no longer planar; the MP2/cc-PVTZ angles O7−C2···C1−S5, O8−C3···C2−S6, and O9−C3···C1−S5 are 42°, 29°, and 29°, respectively.

In a third C_1 barrel-like structure located on the PES (III), the two OCS monomers adopt a parallel (i.e., dipole-aligned) orientation.

The C_s structures IV−VI resemble the C_{3h} cyclic planar structure reported for the $(CO_2)_3$ trimer, with the lowering in symmetry associated with the presence of two different monomer units in $(OCS)_2 \cdot CO_2$. In both structures two of the monomers units adopt a slipped near parallel orientation with the third monomer forming a nearly G-shaped structure with them (see Figure 1). In the case of isomer IV, the two nearly parallel monomers are $OCS \cdot CO_2$ with the sulfur atom closest to the carbon atom of CO_2, which is the geometric disposition leading to the most stable isomer in the isolated dimer. (See $OCS \cdot CO_2$(a) in Table 2.) For isomer V the two nearly parallel monomers are OCS·OCS (dipole antialigned) and its geometric disposition is similar to that adopted by the lowest energy conformation of the isolated dimer [see OCS·OCS(a) in Table 1]. Structure VI has two OCS dipole monomers aligned in a way similar to that in the computed OCS·OCS(c) dimer (see Table 1).

Table 3 lists the structural parameters (bond lengths and angles) obtained at the MP2/cc-pVTZ theoretical level for the six isomers of the $(OCS)_2 \cdot CO_2$ trimer; the corresponding experimental values reported by Peebles and Kuczkowski[10] are also included in this table. As mentioned previously when commenting on Figure 1, the MP2 structural predictions are essentially independent of the basis set employed. Inspection of Table 3 leads to the conclusion that isomer I is clearly the one corresponding to the experimentally detected structure in the microwave spectroscopic studies.[10] Particularly, the geometric parameters computed at the MP2/cc-pVTZ level represent a reasonably good estimate of the experimental values. Indeed, Peebles and Kuczkowski stressed that, apart from the statistical uncertainties arising from the fitting process, the experimental data are obtained ignoring any vibrational contribution to the moments of inertia. These authors concluded that it is reasonable to assume that the equilibrium parameters (i.e., those to be compared with the theoretical estimates) would fall within ±0.05 Å and ±5° of the values given in the first column (exptl) of Table 3. Table 4 fully corroborates this conclusion as the MP2 rotational constants for structure I are the ones closer to the experimental values. On the other hand, the MP2/aug-cc-pVDZ and MP2/cc-pVTZ estimates of the dipole moment (0.476 and 0.419 D, respectively) represent excellent approximations to the experimental value [0.50(4) D].

Table 5 lists the stabilization energies for the six structures I−VI. In agreement with Bone's observation,[51] the 6-31G(d,p) basis set fails to predict structure I as the most stable one. At the MP2 level, the rest of the bases make the correct prediction. At the QCISD(T)//MP2 level, however, the cc-pVDZ basis set gives structure II as the most stable one. The inclusion of diffuse functions (aug-cc-pVDZ) works in the appropriate direction, predicting similar stabilization energies for structures I and II. There is no doubt that in the present case the BSSE must be a crucial factor in determining the correct ordering for the stabilization energies.[18] Unfortunately, the ambiguity associated with the use of the three-body CP recipe to correct for BSSE[41] does not help clarify the situation.

The CBS extrapolation technique[26] provides us with a tool to generate BSSE-free energy predictions. As the CBS-MP4SDTQ and CBS-QCISD(T) levels are computationally impractical at present, we carried out CBS-MP2/cc-pVXZ (X = D, T, Q) calculations to obtain BSSE-free estimates of the stabilization energies for structures I−VI. Feller and Peterson[54] have concluded in recent benchmark studies that the estimate of the CBS limit at the MP2/cc-pVXZ (X = D, T, Q) level by using a combined exponential/Gaussian function has a profound effect on improving the level of agreement with experiment. Although eq 1 is merely a convenient phenomenological function, it has been shown[35] that the CBS extrapolations do not depend heavily on the functional form involved. Therefore, we do believe that the CBS-MP2/cc-pVXZ (X = D, T, Q) energetic estimates are more reliable than the BSSE uncorrected QCISD(T)//MP2 ones. The CBS-MP2 calculations suggest that structure I is the most stable one (D_e = 1760 cm^{-1}), which is consistent with the fact that isomer I is the only one observed in the microwave experiments carried out by Peebles and Kuczkowski. However, the remaining structures II−VI, with CBS-MP2 stabilization energies of 1514, 1660, 1325, 1556, and 1398 cm^{-1}, respectively, are energetically close enough that they might well be present in the molecular beam.

Indeed, in a recent study on a similar system $[OCS \cdot (CO_2)_2]$,[8] the above authors comment that the possibility of identifying other isomeric forms is still an open question. The case of the parent $(CO_2)_3$ trimer, where two different isomers (a barrel-like and a cyclic structure, respectively) were detected in subsequent spectroscopic studies,[55,56] provides us with a representative example supporting such expectations. It is well-known that the carrier gas can have a dramatic role in

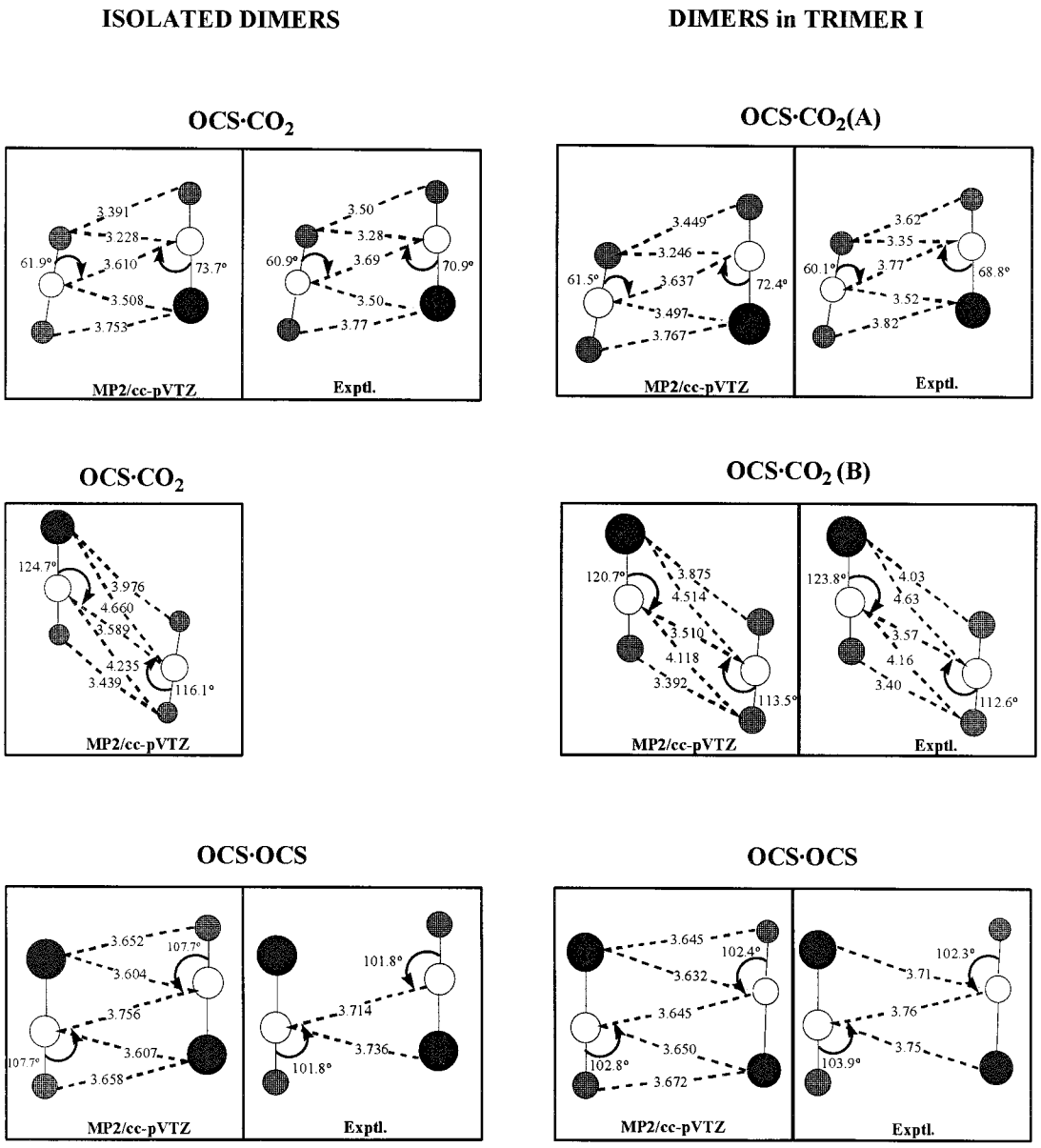

Figure 2. Experimental and theoretical (MP2/cc-pVTZ) geometries for the three dimer faces of structure I (see Figure 1) of the $(OCS)_2$·CO_2 van der Waals complex. The experimental (when available) and theoretical (MP2/cc-pVTZ) geometries of the corresponding isolated dimers are also included for comparison purposes. (See the text for details on the theoretical predictions of two OCS·CO_2 structures with similar energies.) Distances are given in angstroms and angles in degrees.

determining the relative concentrations of conformers of weakly bound complexes in supersonic expansions.[57] Thus, the heavier inert gas atoms (e.g., argon) make the relaxation mechanism which converts the higher energy forms into the most stable species be much more effective than when a lighter inert gas atom (e.g., helium) is used as a carrier gas. The present calculations suggest that further experimental work looking for the detection of other isomers (II−VI) of $(OCS)_2$·CO_2 might be fruitful. The structural information arising from the present study (see Figure 1, Tables 3 and 4, and Supporting Information) should be useful in the initial assignments of the rotational spectra.[10]

Peebles and Kuczkowski used two different semiempirical approaches to make geometric and energetic predictions for the $(OCS)_2$·CO_2 molecular association. While a sophisticated model, employing distributed multipole moments to describe the electrostatic contributions and including an analytical dispersion and repulsion terms by means of an exp−6 expression,[23] yielded excellent structural predictions for the experimentally detected isomer, a hard-sphere repulsion model including only electrostatic and repulsion contributions led to a very poor prediction. These results clearly suggest that the inclusion of dispersion is mandatory for dealing with this type of system. The SAPT analysis presented in the next section fully confirms this point (see Tables 6 and 7). Furthermore, such an analysis will show that the induction forces (not considered in that semiempirical intermolecular interaction potential) also play a relevant role. The stabilization energy predicted by Stone's model[23] (1591.7 cm^{-1})[10] is not far from the CBS-MP2 estimate (1760 cm^1), thus confirming the reliability of that model. However, as for any semiempirical model, the determination of the appropriate parameters could become a major problem. As reported for the case of the $(OCS)_3$ trimer,[58] those parameters that are appropriate for predicting accurate dimer structures are not necessarily appropriate for trimers.

TABLE 5: Stabilization Energies (D_e; kcal/mol and cm^{-1} in Parentheses) for the $(OCS)_2 \cdot CO_2$ van der Waals Complexes[a]

	structure I			structure II			structure III		
basis	MP2	MP4SDTQ[c]	QCISD(T)[c]	MP2	MP4SDTQ[c]	QCISD(T)[c]	MP2	MP4SDTQ[c]	QCISD(T)[c]
6-31G(d,p)	4.3 (1520)	4.5 (1566)	3.7 (1299)	4.9 (1725)	5.1 (1798)	4.8 (1674)	4.4 (1556)	4.6 (1606)	3.9 (1364)
cc-pVDZ	4.3 (1506)	4.3 (1516)	3.6 (1273)	4.1 (1438)	4.3 (1498)	4.0 (1411)	4.3 (1501)	4.3 (1521)	3.7 (1295)
aug-cc-pVDZ	6.2 (2164)	6.5 (2275)	5.5 (1917)	5.7 (1977)	6.2 (2164)	5.5 (1918)	6.0 (2084)	6.3 (2211)	5.4 (1878)
cc-pVTZ	4.7 (1644)			4.3 (1512)			4.5 (1587)		
cc-pVQZ[b]	4.9 (1716)			4.3 (1514)			4.7 (1633)		
CBS	5.0 (1760)			4.3 (1514)			4.7 (1660)		
	structure IV			structure V			structure VI		
basis	MP2	MP4SDTQ[c]	QCISD(T)[c]	MP2	MP4SDTQ[c]	QCISD(T)[c]	MP2	MP4SDTQ[c]	QCISD(T)[c]
6-31G(d,p)	3.7 (1284)	3.8 (1344)	3.3 (1143)	3.9 (1374)	4.1 (1438)	3.5 (1226)	3.6 (1256)	3.7 (1293)	3.1 (1093)
cc-pVDZ	3.7 (1282)	3.8 (1325)	3.2 (1134)	3.9 (1358)	4.0 (1390)	3.4 (1196)	3.7 (1305)	3.7 (1309)	3.2 (1113)
aug-cc-pVDZ	4.9 (1700)	5.2 (1811)	4.5 (1573)	5.4 (1905)	5.7 (1984)	4.9 (1726)	5.0 (1742)	5.1 (1794)	4.4 (1548)
cc-pVTZ	3.6 (1273)			4.1 (1427)			3.7 (1301)		
cc-pVQZ[b]	3.7 (1305)			4.3 (1506)			3.9 (1359)		
CBS	3.8 (1325)			4.4 (1556)			4.0 (1398)		

[a] See Figure 1 for structures I−VI. [b] MP2/cc-pVQZ//MP2/cc-pVTZ calculations. [c] MP4SDTQ//MP2 and QCISD(T)//MP2 calculations.

Nature of the Interactions in the Trimers. The nature of the bonding in structures I−VI was characterized by using a Bader topological analysis of the corresponding charge densities (see Supporting Information for more details). Besides the six intramolecular bond critical points corresponding to the covalent bonds in the monomers (two per monomer), we located three intermolecular bond critical points and one ring critical point for each structure. All the above gives a total of 9 nuclei, 9 bond paths, 1 ring, and 0 cages, thus defining a *characteristic set* (9,9,1,0) for the six structures I−VI which fulfills the Poincaré−Hopf relatioship.[44] The trimer molecular association $(OCS)_2 \cdot CO_2$ is thus formed as a consequence of the existence of three two-body interactions (two $OCS \cdot CO_2$ and one $OCS \cdot OCS$ corresponding to the three intermolecular bond critical points) and one three-body interaction (corresponding to the ring critical point). The magnitude (see Supporting Information) of both the electronic densities (0.002−0.008 au) and the Laplacian of electronic densities (0.01−0.03 au) allows us to classify all the intermolecular critical points as weakly bound interactions[45,59] with dispersion forces playing an important role (see below).

Peebles and Kuczkowski concluded[10] that the $(OCS)_2 \cdot CO_2$ trimer may be described as having two dimer-like interactions that display minimal deviations from their respective dimer structures ($OCS \cdot CO_2$ and $OCS \cdot OCS$) and another $OCS \cdot CO_2$ interaction which is markedly different from that seen in the dimer. It is hard to speculate about the reasons why a given $OCS \cdot CO_2$ dimer interaction can be partly responsible for the formation of a trimer without being capable of forming an isolated dimer. We will see how the theoretical treatment in this work sheds some light on this fundamental point.

Figures 2−5 present under the heading Dimers in Trimer(s) the geometric dispositions of the three dimer faces in each trimer structure (I−VI) as computed at the MP2/cc-pVTZ level and, in the case of structure I (the experimentally observed one), as deduced from the microwave spectroscopic studies.[10] The geometries of the isolated dimers were computed at the MP2/cc-pVTZ level. If available, the corresponding experimental data are also presented in Figures 2−5 for comparison purposes.

In full agreement with Peebles and Kuczkowski's observation,[10] two of the dimer faces in the trimer [the $OCS \cdot OCS$ one and that denoted $OCS \cdot CO_2$(A) in Figure 2] compare rather well with the experimentally observed $OCS \cdot OCS$ and $OCS \cdot CO_2$ isolated dimmers.[52,53] [See $OCS \cdot OCS$(a) and $OCS \cdot CO_2$(a) in Tables 1 and 2. It should be born in mind that "A" and "B" are used to distinguish the two $OCS \cdot CO_2$ dimer faces in the trimer and "a", "b", and "c" denote different isomers of the isolated dimers $OCS \cdot OCS$ and $OCS \cdot CO_2$.] The important point that the

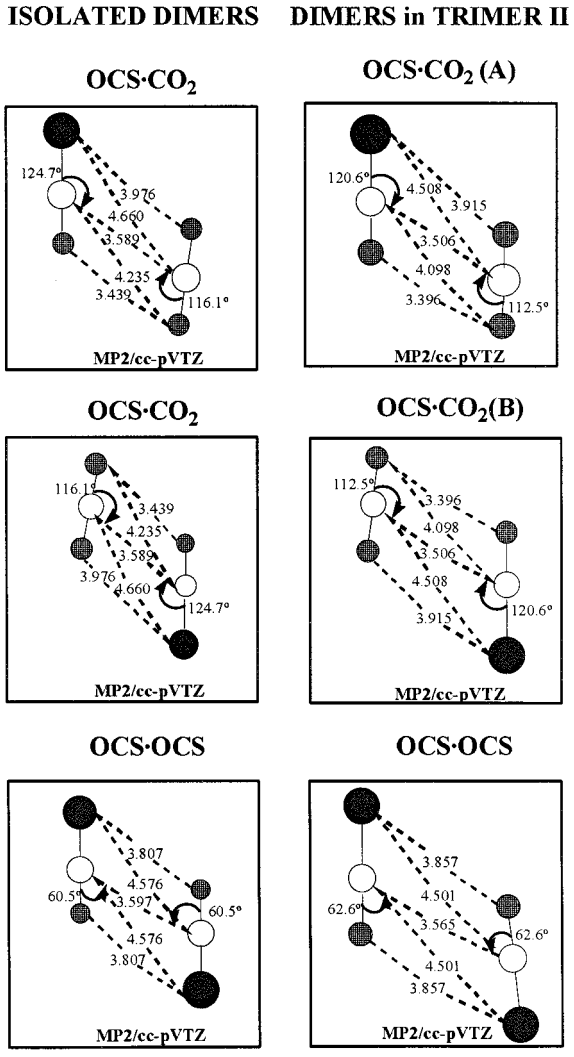

Figure 3. Experimental and theoretical (MP2/cc-pVTZ) geometries for the three dimer faces of structure II (see Figure 1) of the $(OCS)_2 \cdot CO_2$ van der Waals complex. The experimental (when available) and theoretical (MP2/cc-pVTZ) geometries of the corresponding isolated dimers are also included for comparison purposes (See the text for details on the theoretical predictions of two $OCS \cdot CO_2$ and two $OCS \cdot OCS$ structures with similar energies.) Distances are given in angstroms and angles in degrees.

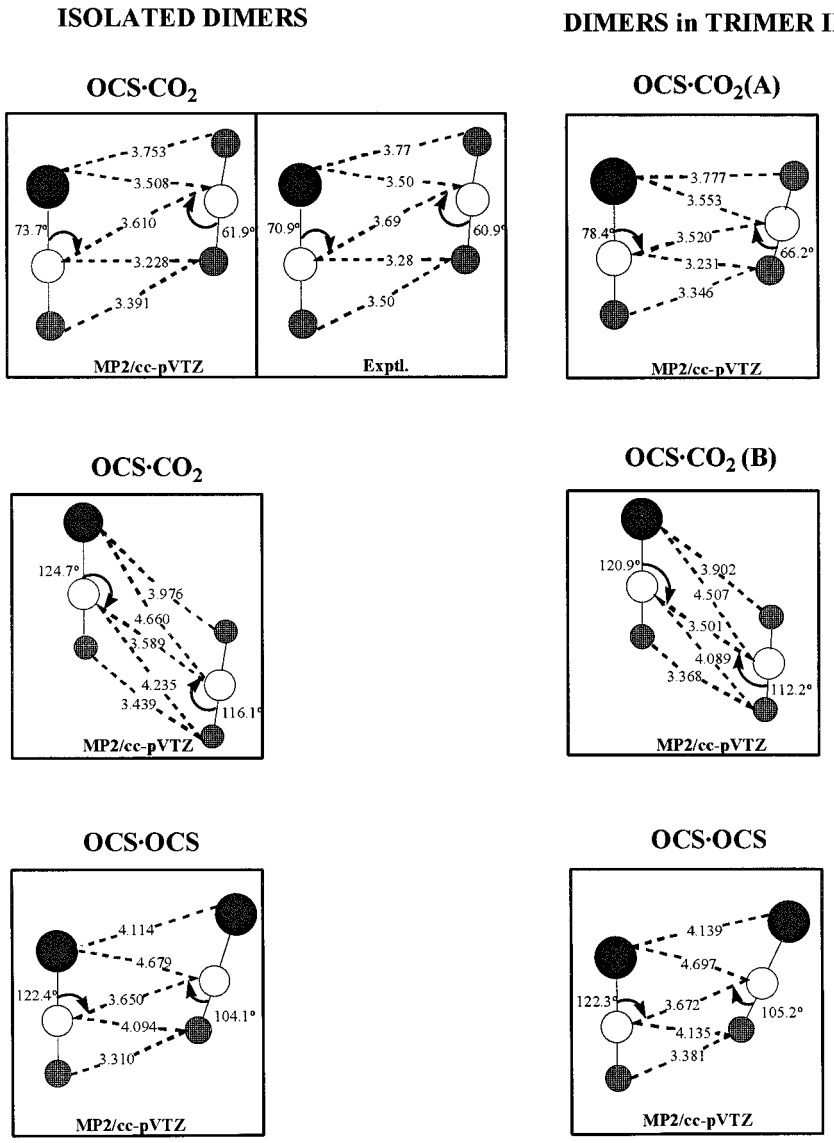

Figure 4. Experimental and theoretical (MP2/cc-pVTZ) geometries for the three dimer faces of structure III (see Figure 1) of the $(OCS)_2$·CO_2 van der Waals complex. The experimental (when available) and theoretical (MP2/cc-pVTZ) geometries of the corresponding isolated dimers are also included for comparison purposes. Distances are given in angstroms and angles in degrees.

present theoretical analysis makes clear is the fact that the third dimer face in the trimer [that denoted as OCS·CO_2(B) in Figure 2] corresponds to the isolated dimer structure OCS·CO_2(b) in Table 2. It should be recalled that such a structure represents a slightly less stable isomer than OCS·CO_2(a) which is the only detected structure in Novick et al.'s microwave spectroscopic studies.[52] Bearing in mind that the MP2/cc-pVTZ stabilization energies of the two structures, OCS·CO_2(a) and OCS·CO_2(b), differ by only 26 cm^{-1} (see Table 2), it seems reasonable to speculate that, as reported for other systems,[17,18,60,61] both isomers are present in the molecular beam and that an appropriate selection of the carrier gas[57] might well lead to the detection of the second isomer. Furthermore, the three dimer faces in structure II (see Figure 3) correspond to those unobserved conformations of the isolated dimers OCS·OCS(b) and OCS·CO_2(b) in Tables 1 and 2. Figure 4 shows that one of the dimer faces in trimer III [OCS·CO_2(A)] corresponds to the experimentally observed dimer OCS·CO_2(a)[52] while the remaining two faces [OCS·CO_2(B) and OCS·OCS] resemble the experimentally unobserved dimer structures OCS·CO_2(b) and OCS·OCS(c), respectively.

In the case of the cyclic C_s trimers IV and V (Figure 5), the two slipped near parallel structures OCS·CO_2(A) and OCS·OCS closely resemble the geometric disposition of the lowest energy isolated dimers OCS·CO_2(a) and OCS·OCS(a) in Tables 1 and 2. The C_s slipped near parallel structure OCS·OCS in VI looks similar to the OCS·OCS(c) dimer structure in Table 1.

Thus the conclusion by Peebles and Kuczkowski[10] that the trimers are composed of dimer-like structures seems to be correct but includes those dimer structures that can remain undetected in the spectroscopic studies despite having stabilization energies quite close to the lowest energy isomers.

Tables 6 and 7 list the different dimer contributions to the total interaction energy of the six trimers I−VI as estimated when using the SAPT approach (eqs 2−4). The corresponding contributions for the OCS·OCS(a), OCS·OCS(b), OCS·OCS(c), OCS·CO_2(a), and OCS·CO_2(b) isolated dimers (see Tables 1 and 2), which according to the previous discussion are the geometric dispositions adopted by some of the dimer faces of the trimer, are also included for comparison purposes.

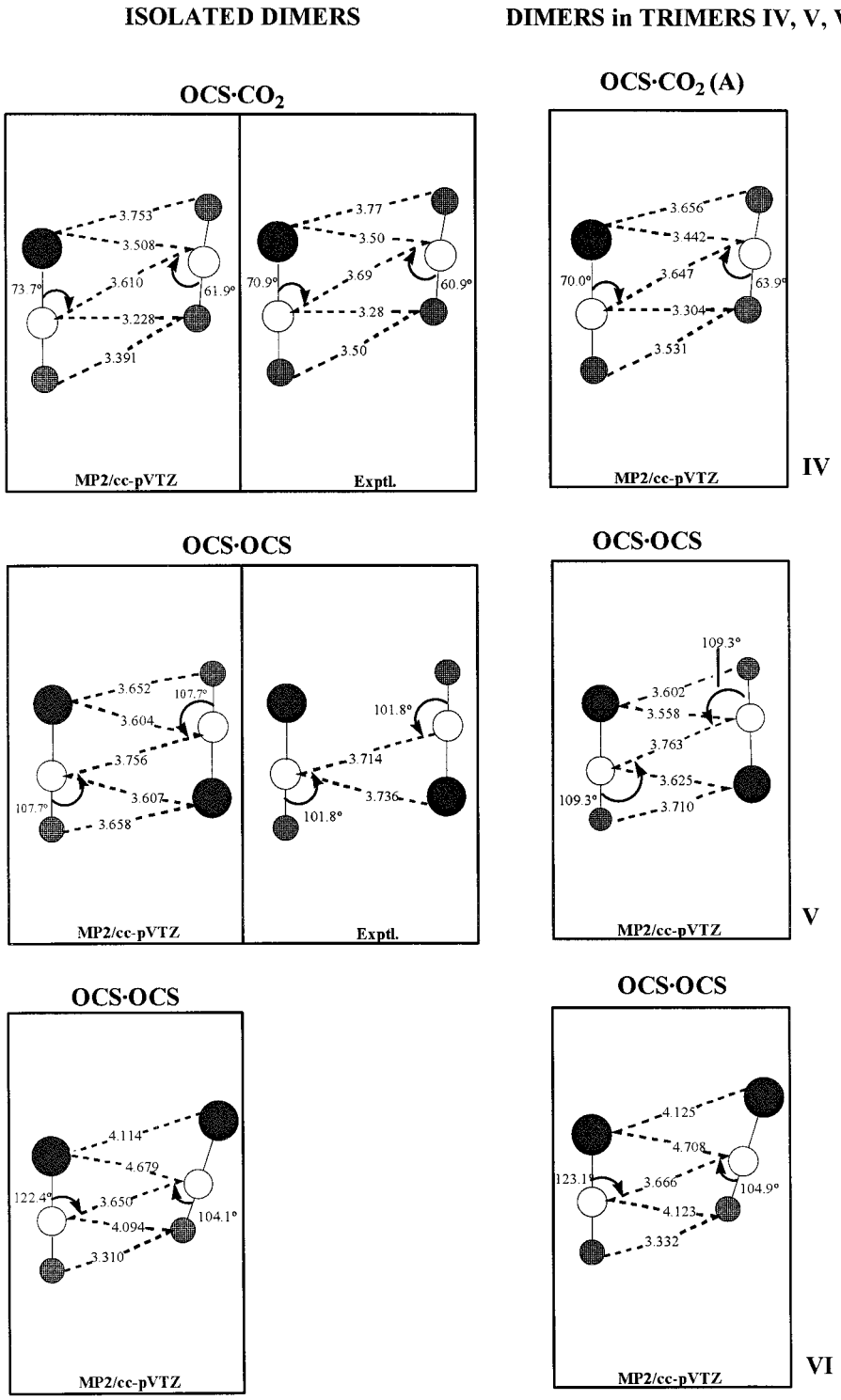

Figure 5. Experimental and theoretical (MP2/cc-pVTZ) geometries for the only slipped near parallel dimer face in the three planar structures IV−VI (see Figure 1) of the $(OCS)_2 \cdot CO_2$ van der Waals complex. The experimental (when available) and theoretical (MP2/cc-pVTZ) geometries of the corresponding isolated dimers are also included for comparison purposes. Distances are given in angstroms and angles in degrees.

It is clear from Tables 6 and 7 that the nature of the interactions in the three isolated dimers OCS·OCS(a), OCS·OCS(b), and OCS·OCS(c) is quite different. Indeed, the attractive forces (polarization, induction, and dispersion) in the lowest energy isomer [OCS·OCS(a)] are notably greater (absolute value) than those in the OCS·OCS(b) or OCS·OCS(c) isomers while the exchange contributions (repulsive) are much less important for these latter structures. Thus, we can think of OCS·OCS(a) as a molecular association with a geometry that *maximizes* (M) the attractive components of the interaction energy at the cost of a larger overlap which enhances the repulsive components. Let us denote this type of association as M-complex. By contrast, the OCS·OCS(b) and OCS·OCS(c) geometries seem to *minimize* (m) the repulsions at the expense of a considerable reduction in the attractive forces. Let us denote this type of association as m-complex. Of course, to maximize

TABLE 6: Different Contributions (See Text for Definitions) to the SAPT/aug-cc-pVDZ//MP2/aug-cc-pVDZ Interaction Energies [E_{int}(SAPT)] for the Isolated Dimers and for the Dimer Faces of the Trimers (See Figures 2−5 for Structural Information)[a]

	isolated dimers					structure I			structure II		
	dimer[b] OCS·OCS(a)	dimer[c] OCS·OCS(b)	dimer[c] OCS·OCS(c)	dimer[b] OCS·CO_2(a)	dimer[c] OCS·CO_2(b)	OCS· OCS	OCS· CO_2(A)	OCS· CO_2(B)	OCS· OCS	OCS· CO_2(A)	OCS· CO_2(B)
$E_{pol}^{(10)}$	−742	−446	−584	−611	−560	−556	−646	−486	−381	−469	−469
$E_{pol,r}^{(12)}$	34	96	37	28	127	−44	41	87	46	79	78
$E_{pol}^{(1)}$	−708	−350	−547	−583	−433	−600	−605	−399	−335	−390	−391
$E_{ind,r}^{(20)}$	−835	−282	−601	−657	−303	−741	−703	−318	−271	−310	−312
$^tE_{ind}^{(22)}$	24	−24	0	8	−31	19	10	−31	−29	−32	−32
$E_{ind}^{(2)}$	−811	−306	−601	−649	−334	−722	−693	−349	−300	−342	−344
$E_{disp}^{(20)}$	−1420	−1007	−1257	−1004	−806	−1360	−1009	−857	−1020	−837	−840
$E_{disp}^{(2)}$	−1420	−1007	−1257	−1004	−806	−1360	−1009	−857	−1020	−837	−840
$E_{exch}^{(10)}$	1413	806	1168	1080	748	1310	1124	794	815	776	779
$E_{exch}^{(11)} + E_{exch}^{(12)}$	35	113	71	81	123	35	76	128	109	128	129
$E_{exch}^{(1)}$	1448	919	1239	1161	871	1345	1200	922	924	904	908
$E_{exch-ind,r}^{(20)}$	775	225	538	560	224	688	604	235	220	229	230
$^tE_{exch-ind,r}^{(22)}$	−22	19	0	−7	23	−18	−8	23	24	24	24
$E_{exch-disp}^{(20)}$	162	78	125	103	64	151	107	68	79	66	66
$E_{exch}^{(2)}$	915	322	663	656	311	821	703	326	323	319	320
E_{int}^{HF}	543	254	462	333	81	641	340	189	342	193	197
E_{int}^{CORR}	−1188	−725	−1024	−790	−499	−1216	−784	−581	−791	−572	−575
E_{int}(SAPT)	−645	−472	−561	−458	−418	−576	−444	−392	−450	−379	−378
E_{int}^{SUP}(NCP)	−888	−698	−788	−691	−631	−803	−670	−610	−677	−596	−596
E_{int}^{SUP}(CPR)	−559	−419	−489	−399	−373	−496	−382	−339	−392	−328	−327

[a] The corresponding MP2/aug-cc-pVDZ interaction energies with [E_{int}^{SUP}(CPR)] and without [E_{int}^{SUP}(NCP)] the CP corrections (including fragment relaxation terms) for the BSSE are also given. All numbers are given in cm^{-1}. [b] MP2/aug-cc-pVDZ geometric disposition corresponding to the experimentally detected geometries (see refs 52 and 53 and Tables 1 and 2). [c] MP2/aug-cc-pVDZ geometric disposition corresponding to a theoretically predicted structure whose energy is quite close to the experimentally detected geometry.

TABLE 7: Different Contributions (See Text for Definitions) to the SAPT/aug-cc-pVDZ//MP2/aug-cc-pVDZ Interaction Energies [E_{int}(SAPT)] for the Isolated Dimers and for the Dimer Faces of the Trimers (See Figures 2−5 for Structural Information)[a]

	structure III			structure IV			structure V			structure VI		
	OCS· OCS	OCS· CO_2(A)	OCS· CO_2(B)	OCS· OCS	OCS· CO_2(A)	OCS· CO_2(B)	OCS· OCS	OCS· CO_2(A)	OCS· CO_2(B)	OCS· OCS	OCS· CO_2(A)	OCS· CO_2(B)
$E_{pol}^{(10)}$	−592	−452	−472	−401	−679	−356	−780	−464	−398	−614	−382	−401
$E_{pol,r}^{(12)}$	42	−42	82	38	50	65	42	93	35	48	32	38
$E_{pol}^{(1)}$	−550	−494	−390	−363	−629	−291	−738	−371	−363	−566	−350	−363
$E_{ind,r}^{(20)}$	−607	−603	−314	−225	−765	−154	−880	−163	−209	−629	−398	−209
$^tE_{ind}^{(22)}$	−1	5	−31	−30	16	−14	25	−19	−28	2	−3	−30
$E_{ind}^{(2)}$	−608	−598	−345	−255	−749	−168	−855	−182	−237	−627	−401	−239
$E_{disp}^{(20)}$	−1238	−990	−846	−642	−1006	−607	−1449	−563	−554	−1257	−657	−559
$E_{disp}^{(2)}$	−1238	−990	−846	−642	−1006	−607	−1449	−563	−554	−1257	−657	−559
$E_{exch}^{(10)}$	1167	1032	781	599	1156	501	1475	493	566	1190	658	564
$E_{exch}^{(11)} + E_{exch}^{(12)}$	67	82	130	81	66	76	33	114	67	65	47	68
$E_{exch}^{(1)}$	1234	1114	911	680	1222	577	1508	607	633	1255	705	632
$E_{exch-ind,r}^{(20)}$	548	514	230	187	662	127	817	108	174	567	337	172
$^tE_{exch-ind,r}^{(22)}$	1	−4	23	25	−14	12	−23	13	24	−2	3	25
$E_{exch-disp}^{(20)}$	126	98	67	50	111	46	169	39	46	128	61	45
$E_{exch}^{(2)}$	675	608	320	262	759	185	963	160	244	693	401	242
E_{int}^{HF}	459	455	192	107	334	89	562	−51	89	454	188	82
$E_{int,r}^{CORR}$	−1004	−851	−577	−478	−777	−423	−1203	−322	−411	−1015	−518	−414
E_{int}(SAPT)	−544	−396	−385	−371	−443	−334	−641	−373	−322	−560	−330	−331
E_{int}^{SUP}(NCP)	−760	−624	−610	−531	−671	−506	−881	−561	−465	−784	−508	−477
E_{int}^{SUP}(CPR)	−466	−338	−333	−328	−385	−308	−548	−340	−280	−488	−295	−290

[a] The corresponding MP2/aug-cc-pVDZ interaction energies with [E_{int}^{SUP}(CPR)] and without [E_{int}^{SUP}(NCP)] the CP corrections (including fragment relaxation terms) for the BSSE are also given. All numbers are given in cm^{-1}. [b] MP2/aug-cc-pVDZ geometric disposition corresponding to the experimentally detected geometries (see refs 52 and 53 and Tables 1 and 2). [c] MP2/aug-cc-pVDZ geometric disposition corresponding to a theoretically predicted structure whose energy is quite close to the experimentally detected geometry.

the stabilizing contributions and to minimize the repulsive forcesrepresent two complementary ways of optimizing a geometric arrangement of a molecular association. All the above isconsistent with the geometries depicted for these two structures

TABLE 8: Three-Body Contributions (in cm^{-1}) to the Interaction Energy for Structures I−VI as Estimated at Different Theoretical Levels

level	structure I	structure II	structure III	structure IV	structure V	structure VI
MP2/6-31G(d,p)	1	−5	−10	7	−12	10
MP4SDTQ/6-31G(d,p)	7	−6	−5	11	−13	17
QCISD(T)/6-31G(d,p)	8	−38	−6	9	−27	2
MP2/cc-pVDZ	−7	1	−12	0	−10	7
MP4SDTQ/cc-pVDZ	−2	1	−5	3	−8	15
QCISD(T)/cc-pVDZ	11	−22	−3	−1	−17	5
MP2/aug-cc-pVDZ	−81	−108	−96	8	2	27
MP4SDTQ/aug-cc-pVDZ	−78	−116	−96	22	14	38
QCISD(T)/aug-cc-pVDZ	−54	−127	−47	21	3	69
MP2/cc-pVTZ	−39	−44	−46	0	−8	9

in Tables 1 and 2. OCS·OCS(a) is a stacked structure while OCS·OCS(b) is a slipped parallel structure and OCS·OCS(c) is a stacked structure but with the sulfur atoms significantly separated. Similar considerations apply to the OCS·CO_2(a) and OCS·CO_2(b) isolated dimer structures.

The analysis of the SAPT components for structure I (see Table 6) shows that the nature of the interactions in the OCS·OCS fragment is rather similar to the one previously described for the OCS·OCS(a) isolated dimer (M-complex). On the other hand, while the OCS·CO_2(A) fragment is an M-complex, the OCS·CO_2(B) fragment can be classified as an m-complex. Thus, trimer I composed of the OCS·OCS, OCS·CO_2(A), and OCS·CO_2(B) faces can be viewed as an MMm-complex. Inspection of Table 6 shows that structures II and III can be classified as mmm- and mMm-complexes, respectively. In the case of the planar isomer IV, Table 7 shows that the OCS·CO_2(A) fragment is an M-complex. The other two faces [OCS·CO_2(B) and OCS·OCS fragments], characterized by very small attractive and repulsive contributions, are not associated with any minimum in their respective PESs. This is fully confirmed by comparing the quasi-T-shaped structure of the OCS·CO_2(B) fragment and the quasi-G-shaped structure of the OCS·OCS fragment in Figure 1 with the corresponding (optima) slipped near parallel dimer structures shown in Tables 1 and 2. A similar analysis applies to the planar isomers V and VI for which the OCS·OCS fragments correspond to M- and m-complex, respectively, and the remaining faces adopt very weakly interacting quasi-T-shaped and quasi-G-shaped orientations (see Figure 1).

In a recent paper,[8] Peebles and Kuczkowski concluded that although the induction interaction forces are not included in the Stone semiempirical potential[23] they employed, their contribution is expected to be small in this type of systems. Tables 6 and 7 show that the induction contributions, as estimated by SAPT, are similar in magnitude to the electrostatic contributions.

Let us now make a short comment on the two-body BSSE contributions. Tables 6 and 7 collect, in addition to E_{int}(SAPT) (the BSSE-free SAPT estimate of the dimer interaction energies), the corresponding uncorrected [E_{int}^{SUP}(NCP)] and CP corrected [E_{int}^{SUP}(CPR)] supermolecular estimates (this latter value computed by including fragment relaxation terms).[62] Two important conclusions emerge from inspection of these three estimates of the total interaction energy:

(a) The MP2/aug-cc-pVDZ CP estimate of the two-body BSSE [BSSE = E_{int}^{SUP}(CPR) − E_{int}^{SUP}(NCP)] is by no means negligible and becomes even greater with the cc-pVTZ triple-ζ basis. Although the uncorrected and CP corrected interaction energies follow, in general, the same trend in such a way that the predictions on the relative stabilities at both levels usually coincide (although this is not always the case),[18] there is no doubt that, to compare the interaction energies with the experimental values, when available (see, e.g., ref 21), consideration of BSSE seems to be mandatory.

(b) In all cases, the BSSE-free E_{int}(SAPT) values are (in absolute value) lower than the corresponding uncorrected ones [E_{int}^{SUP}(NCP)] but higher than the CP corrected values [E_{int}^{SUP}(CPR)]. This result is consistent with the belief (see, for example, refs 16 and 39) that the CP algorithm overcorrects the BSSE at the correlated level.

Bearing in mind the above two points, one can conclude that, in any case, the CP corrected values are always useful as upper limit estimates of the interaction energies.

Before ending we would like to briefly comment on the nonadditive effects. Table 8 collects the three-body contributions to the interaction energy as computed at different theoretical levels for the six $(OCS)_2$·CO_2 isomers considered in the present work. It is clear that whereas the three-body contributions exhibit a quite strong dependence on the basis sets used, they are less sensitive to the theoretical method employed. The QCISD(T)/aug-cc-pVDZ and MP2/cc-pVTZ estimates of the three-body contributions represent a very small part of the total interaction energy. For example, in the case of the most stable structure I, it is 2.4% or 2.8%, respectively, in full agreement with previous findings in similar complexes; a value of 3% was estimated for the $(CO_2)_3$ trimer at the CCSD(T)/aug-6311G(d) level.[63] The aug-cc-pVDZ and cc-pVTZ basis sets show that the three-body contributions are stabilizing for the barrel-like structures (I−III) while they become, in general, less important for the three planar isomers (IV−VI).

Conclusions

The potential energy surface of the $(OCS)_2$·CO_2 molecular association has been extensively explored at the MP2 [using the 6-31G(d,p), cc-PVXZ (X = D, T) and aug-cc-pVDZ basis sets] level of theory. Six minima structures were located: three barrel-like (two C_1 and one C_2 symmetries, respectively) and three planar (C_s symmetry). The MP2 geometric parameters, rotational constants, and dipole moment of one of the barrel-like isomers (C_1 symmetry) agree rather well with the corresponding experimental values for the only structure observed in pulsed-nozzle Fourier transform microwave spectroscopic studies.

The stabilization energies of the six isomers located on the potential energy surface are rather similar, thus suggesting that an appropriate selection of the carrier gas in the supersonic expansion could lead to the experimental detection of some other structures, as in the case of the $(CO_2)_3$ trimer where the existence of two isomers (one noncyclic and one cyclic) has been reported. The structural information provided in the present theoretical study may be helpful to plan further experimental work in that direction.

The six isomers were topologically characterized as structures with six intramolecular bond critical points (corresponding to the covalent bonds), three intermolecular bond critical points (one for each dimer face), and one ring critical point, defining a (9,9,1,0) *characteristic set*. The many-body symmetry-adapted perturbation theory showed that, in the barrel-like structures, the dimer faces tend to adopt geometric dispositions that resemble the optimum conformations predicted for the isolated dimers. Some of these dimer arrangements correspond to the geometries detected in spectroscopic studies on the dimer species, but some others represent alternate undetected isomers characterized as minima on the potential energy surface, with stabilization energies similar to the ones of the observed structures. Thus, theoretical explorations on the existence of stable dimer associations (not necessarily detected in the spectroscopic studies) can be helpful to rationalize the trimer or larger cluster geometries.

The dispersion forces make the most important attractive contributions to the interaction energies of the six structures located and, despite the small dipole moments involved, the induction interaction forces make contributions similar in magnitude to those of the electrostatic forces.

The three-body contributions are small and stabilizing for the barrel-like structures and become, in general, less important for the planar isomers.

Acknowledgment. The authors thank Prof. Fraga for a critical reading of the manuscript and Prof. A. Martín Pendás for helpful comments on the use of Bader's methodology to analyze the charge density. Partial financial support by DGES (Madrid, Spain) under Project No. PB97-0399-C03-03 is greatly acknowledged.

Supporting Information Available: MP2/cc-pVTZ Cartesian coordinates, Bader's bond properties, and B3LYP/6-31G(d,p) geometric and energetic parameters for the six structures I−VI. This material is available free of charge via the Internet at http://pubs.acs.org.

References and Notes

(1) Castleman, A. W., Jr.; Bowen, K. H., Jr *J. Phys. Chem*. **1996**, *100*, 12911.
(2) Yarkony, D. R., Ed.; *Modern Electronic Structure Theory*; World Scientific: Singapore, 1995; Parts I and II.
(3) Bacic, Z.; Miller, R. E. *J. Phys. Chem*. **1996**, *100*, 12945.
(4) Alivisatos, A. P. *J. Phys. Chem*. **1996**, *100*, 13226.
(5) . *Chem. Rev*. **1988**, *88*, 813−988.
(6) . *Chem. Rev*. **1994**, *94*, 1721−2160.
(7) . *Chem. Rev*. **2000**, *100*, 3861−4264.
(8) See: Peebles, S. A.; Kuczkowski, R. L *J. Chem. Phys*. **1998**, *109*, 5276 and references therein.
(9) Peebles, S. A.; Kuczkowski, R. L. *J. Mol. Struct. (THEOCHEM)* **1998**, *447*, 151.
(10) Peebles, S. A.; Kuczkowski, R. L *J. Phys. Chem. A* **1998**, *102*, 8091.
(11) Chalasinski, G.; Szczesniak, M. M. *Chem. Rev*. **2000**, *100*, 4227.
(12) Hehre, W. J.; Radom, L.; Schleyer, P. v. R.; Pople, J. A. *Ab initio Molecular Orbital Theory*; Wiley: New York, 1986.
(13) Bartlett, R. J.; Stanton, J. F. *Reviews in Computational Chemistry*; VCH: New York, 1994; Vol. 5.
(14) Jeziorski, B.; Moszynski, R.; Szalewicz, K. *Chem. Rev*. **1994**, *94*, 1887.
(15) Valdés, H.; Rayón, V. M.; Sordo, J. A. *Chem. Phys. Lett*. **1999**, *309*, 265.
(16) López, J. C.; Alonso, J. L.; Lorenzo, F. J.; Rayón, V. M.; Sordo, J. A. *J. Chem. Phys*. **1999**, *111*, 6363.
(17) Valdés, H.; Rayón, V. M.; Sordo, J. A. *Chem. Phys. Lett*. **2000**, *320*, 507.
(18) Valdés, H.; Sordo, J. A. *Chem. Phys. Lett*. **2001**, *333*, 169.
(19) Rayón, V. M.; Sordo, J. A. *J. Phys. Chem. A* **1997**, *101*, 7414.
(20) Rayón, V. M.; Sordo, J. A. *J. Chem. Phys*. **1997**, *107*, 7912.
(21) Rayón, V. M.; Sordo, J. A. *J. Chem. Phys*. **1999**, *110*, 377.
(22) Rayón, V. M.; Sordo, J. A. *Chem. Phys. Lett*. **2001**, *341*, 575.
(23) Stone, A. J.; Dullweber, A.; Hodges, M. P.; Popelier, P. L. A.; Wales, D. J. *ORIENT: A program for studying interactions between molecules*, Version 3.2; University of Cambridge: 1995.
(24) Dunning, T. H., Jr. *J. Chem. Phys*. **1989**, *90*, 1007.
(25) Kendall, R. A.; Dunning, T. H., Jr. *J. Chem. Phys*. **1992**, *96*, 6796.
(26) Dunning, T. H., Jr. *J. Phys. Chem. A* **2000**, *104*, 9062.
(27) Sponer, J.; Hobza, P. *J. Phys. Chem. A* **2000**, *104*, 4592.
(28) Rappé, A. K.; Bernstein, E. R. *J. Phys. Chem. A* **2000**, *104*, 6117.
(29) Becke, A. D. *J. Chem. Phys*. **1992**, *97*, 9173.
(30) Lee, C.; Yang, W.; Parr, R. G. *Phys. Rev. B* **1988**, *37*, 785.
(31) Müller-Dethlefs, K.; Hobza, P. *Chem. Rev*. **2000**, *100*, 143.
(32) Stone, A. J. *The Theory of Intermolecular Forces*; Clarendon Press: Oxford, 1996.
(33) Jensen, F. *Introduction to Computational Chemistry*; Wiley: Chichester, 1999.
(34) Feller, D.; Sordo, J. A. *J. Chem. Phys*. **2000**, *112*, 5604.
(35) Feller, D.; Sordo, J. A. *J. Chem. Phys*. **2000**, *113*, 485.
(36) Sordo, J. A. *J. Chem. Phys*. **2001**, *114*, 1974.
(37) Boys, S. F.; Bernardi, F. *Mol. Phys*. **1970**, *19*, 553.
(38) Van Duijneveldt, F. B.; van Duijneveldt, J. G. C. M.; van Lenthe, J. H. *Chem. Rev*. **1994**, *94*, 1873.
(39) See ref 16 for a few illustrative references on the subject. Conclusive data supporting the overcorrection of the CP algorithm are given in: Timoshkin, A. Y.; Suvorov, A. V.; Bettinger, H. F.; Schaefer, H. F., III. *J. Am. Chem. Soc*. **1999**, *121*, 5687.
(40) . Bukowski, R.; Jankowski, P.; Jeziorski, B.; Jeziorski, M.; Kucharski, S. A.; Moszynski, R.; Rybak, S.; Szalewicz, K.; Willians, H. L.; Wormer, P. E. S. *SAPT96: An ab initio Program for Many-Body Symmetry-Adapted Perutbation Theory Calculations of Intermolecular Interaction Energies*; University of Delaware and University of Warsaw: 1996.
(41) Lendvay, G.; Mayer, I. *Chem. Phys. Lett*. **1998**, *297*, 365.
(42) Peterson, K. A.; Woon, D. E.; Dunning, T. H., Jr. *J. Chem. Phys*. **1994**, *100*, 7410.
(43) Frisch, M. J.; Trucks, G. W.; Schlegel, H. B.; Scuseria, G. E.; Robb, M. A.; Cheeseman, J. R.; Zakrzewski, V. G.; Montgomery, J. A., Jr.; Stratmann, R. E.; Burant, J. C.; Dapprich, S.; Millan, J. M.; Daniels, A. D.; Kudin, K. N.; Strain, M. C.; Farkas, O.; Tomasi, J.; Barone, V.; Cossi, M.; Cammi, R.; Mennucci, B.; Pomelly, C.; Adamo, C.; Clifford, S.; Ochterski, J.; Petersson, G. A.; Ayala, P. Y.; Cui, Q.; Morokuma, K.; Malick, D. K.; Rabuck, A. D.; Raghavachari, K.; Foresman, J. B.; Cioslowski, J.; Ortiz, J. V.; Baboul, A. G.; Stefanov, B. B.; Liu, G.; Liashenko, A.; Piskorz, P.; Komaromi, I.; Gomperts, R.; Martin, R. L.; Fox, D. J.; Keith, T.; Al-Laham, M. A.; Peng, C. Y.; Nanayakkara, A.; Gonzalez, C.; Challacombe, M.; Gill, P. M. W.; Johnson, B.; Chen, W.; Wong, M. W.; Andres, J. L.; Head-Gordon, M.; Replogle, E. S.; Pople, J. A. *Gaussian 98*; Gaussian Inc.: Pittsburgh, PA, 1998.
(44) Bader, R. F. W. *Atoms in Molecules. A Quantum Theory*; Oxford University Press: New York, 1990.
(45) Bone, R. G.; Bader, R. F. W. *J. Chem. Phys*. **1996**, *100*, 10892.
(46) Chalasinski, G.; Jeziorski, B. *Theor. Chim. Acta* **1977**, *46*, 277.
(47) Szalewicz, K.; Jeziorski, B. *Mol. Phys*. **1979**, *38*, 191.
(48) Bewish, R. J.; Oudejans, L.; Miller, R. E.; Moszynski, R.; Heijmen, T. G. A.; Wormer, P. E. S.; van der Avoird, A. *J. Chem. Phys*. **1998**, *109*, 8968.
(49) Misquitta, A. J.; Bukowski, R.; Szalewicz, K. *J. Chem. Phys*. **2000**, *112*, 5308.
(50) Chalasinski, G.; Szczesniak, M. M. *Mol. Phys*. **1988**, *63*, 205.
(51) Bone, R. G. A. *Chem. Phys. Lett*. **1993**, *206*, 260.
(52) Novick, S. E.; Suenram, R. D.; Lovas, F. J. *J. Chem. Phys*. **1988**, *88*, 687.
(53) Randall, R. W.; Wilkie, J. M.; Howard, B. J.; Muenter, J. S. *Mol. Phys*. **1990**, *69*, 839.
(54) Feller, D.; Peterson, K. A. *J. Chem. Phys*. **1998**, *108*, 154.
(55) Weida, M. J.; Sperhac, J. M.; Nesbitt, D. J. *J. Chem. Phys*. **1995**, *103*, 7685.
(56) Weida, M. J.; Nesbitt, D. J. *J. Chem. Phys*. **1996**, *105*, 10210.
(57) Rouff, R. S.; Klots, J. D.; Emilsson, T.; Gutowski, H. S. *J. Chem. Phys*. **1990**, *93*, 3142.
(58) Peebles, S. A.; Kuczkowski, R. L. *J. Phys. Chem. A* **1999**, *103*, 6344.
(59) Cremer, D.; Kraka, E. *Angew. Chem*. **1984**, *23*, 627.
(60) Antolínez, S.; López, J. C.; Alonso, J. L. *Angew. Chem., Int. Ed*. **1999**, *38*, 1772.
(61) Sanz, M. E.; López, J. C.; Alonso, J. L. *Chem. Eur. J*. **1999**, *5*, 3293.
(62) See: Rayón, V. M.; Sordo, J. A. *Theor. Chem. Acc*. **1998**, *99*, 68 and references therein.
(63) Tsuzuki, S.; Klopper, W.; Lüthi, H. P. *J. Chem. Phys*. **1999**, *111*, 3846.